A Novel Methodology for Comprehensive Planning of Battery Storage Systems

Paul Arévalo, Marcos Tostado-Véliz, and Francisco Jurado*

Department of Electrical Engineering, University of Jaén, 23700 EPS Linares, Jaén, Spain

ABSTRACT

Battery storage system design has become a crucial task for nanogrids and microgrids planning, as it strongly determines the techno-economic viability of the project. Despite that, most of developed methodologies for optimally planning this kind of systems still present some important issues like high computational burden or insufficient results. This paper develops a novel methodology for battery storage system planning in nanogrids and microgrdis, which aims at overcoming the main issues presented by other methodologies. To achieve this goal, our proposal originally combines different software, clustering techniques and optimization tools. As salient features of the developed approach, it is worth remarking its efficiency, versatility, ability to manage with different time horizons and comprehensiveness. A prospective nanogrid in the region of Cuenca, Ecuador, serves as illustrative case study to show the capabilities, efficiency and effectiveness of the proposed approach as providing sufficient guidelines for its universal applicability. Among other relevant results, our proposal is able to determine that, for the studied grid, the daily operating cost can be reduced up to 17% by using Nickel-Cadmium batteries, however, the usage of Lead-Acid and Sodium-Sulfur technologies resulted more attractive through the project lifetime due to their longer lifetimes and relatively low capital costs.

Keywords: Nanogrid, Battery technologies, Depth of discharge, HOMER Pro, Mixed-Integer Quadratic Programming.

---

*Corresponding author, Tel.: +34 953 648518; Fax: +34 953 648586.
E-mail addresses: fjurado@ujaen.es (F. Jurado), wpac0001@red.ujaen.es (P. Arévalo) mtostado@ujaen.es (M. Tostado-Véliz)

HIGHLIGHTS

- A novel methodology for battery storage system planning in nanogrids and microgrids is developed.
- The developed methodology originally combines different software, techniques and optimization tools in order to overcome the issues presented by other approaches.
- As main features of the developed approach, it is worth remarking its efficiency, versatility, ability to manage with different time horizons and comprehensiveness
- For illustrative purposes, a benchmark case study on a prospective nanogrid in the region of Cuenca, Ecuador, is considered to show the capabilities of the developed framework.

Nomenclature

Acronyms	
NG	Nanogrid
BSS	Battery Storage System
PV	Photovoltaic
O&M	Operation and maintenance
WG	Wind generation
HK	Hydrokinetic
DEG	Diesel engine generator
DOD	Depth of discharge
NPV	Net present value
Li-ion	Lithium-ion
NiCd	Nickel-Cadmium
NaS	Sodium-Sulfur
Sets	
Ψ_R	Set of representative days
Ψ_T	Set of time intervals within the studied time horizon
ρ_r	Number of days within the cluster of the representative day r
Measured data	
$I_{r,t}$	Solar irradiance at representative day r and time t [W/m²]
$T_{r,t}^{cell}$	Cell temperature at representative day r and time t [ºC]
$T_{r,t}$	Temperature at representative day r and time t [ºC]
$V_{r,t}^{W}$	Wind speed at representative day r and time t [m/s]
$V_{r,t}^{RV}$	River speed at representative day r and time t [m/s]
$p_{r,t}^{Demand}$	Local demand at representative day r and time t [kW]
Overall parameters	
g^{PV}	Derating factor of the PV array (0.80)
I_S	Solar irradiance under standard conditions (1000 W/m²)
α^{PV}	Temperature coefficient of power (0.03)

T_S	Temperature under standard conditions (25 ºC)
T_{NOCT}^{C}	Manufacturer report cell temperature under standard conditions (47 ºC)
T_{NOCT}^{A}	Manufacturer report ambient temperature under standard conditions (20 ºC)
I_{NOCT}^{T}	Manufacturer report solar irradiance under standard conditions (800 W/m²)
ρ^{W}	Air density (0.967 kg/m³)
C_p	Power coefficient of a turbine performance (0.42)
ρ^{H_2O}	Water density (997 kg/m³)
$\Delta\tau$	Time step [hrs.]
T	Last time interval of the studied time horizon
Other data	
η^{PV}	Efficiency of the PV array [pu]
η^{WG}	Efficiency of the WG system [pu]
A^{WG}	Turbine swept area of the WG system [m²]
V^{WG}	Rated speed of the WG system [m/s]
$V^{WG,cut-in}/V^{WG,cut-out}$	Cut-in/cut-out speed of the WG system [m/s]
η^{HK}	Efficiency of the HK system [pu]
A^{HK}	Turbine swept area of the HK system [m²]
$V^{HK,cut-in}/V^{HK,cut-off}$	Cut-in/cut-off speed of the HK system [m/s]
RD^{DEG}/RU^{DEG}	Ramp down/up limits of the DEG [kW]
$E2P^{BSS}$	Energy-to-power ratio of the BSS system [hrs.]
DOD^{BSS}	Depth of discharge of the BSS system [pu]
$\eta^{BSS,C}/\eta^{BSS,D}$	Charging/discharging efficiency of the BSS system
ν	Random number
γ	Penalty term [$]
a, b, c	Cost coefficients of the different units

λ	Start-up and shutdown costs [$]

Variables of the planning horizon problem

N^{PV}	No. of panels of the PV array
P^{PV}	Rated power of a PV panel [W]
N^{WG}	No. of wind turbines of the WG system
P^{WG}	Rated power of a wind turbine [W]
N^{HK}	No. of turbines of the HK system
$p^{DEG,min}/p^{DEG,max}$	Min./max. capacity of the DEG [kW]
S^{BSS}	Capacity of the BSS [kWh]

Variables of the operating horizon problem

$p_{r,t}^{PV}$	Power given by the PV system at representative day r and time t [kW]
$p_{r,t}^{WG}$	Power given by the WG system at representative day r and time t [kW]
$p_{r,t}^{HK}$	Power given by the HK system at representative day r and time t [kW]
$p_{r,t}^{DEG}$	Power given by the DEG at representative day r and time t [kW]
$\delta_{r,t}^{DEG}$	Operation status of the DEG at representative day r and time t (1 = ON, 0 = OFF) [Binary]
$p_{r,t}^{BSS,C}/p_{r,t}^{BSS,D}$	Charging/discharging power of the BSS at representative day r and time t [kW]
$\delta_{r,t}^{BSS,C}/\delta_{r,t}^{BSS,D}$	Charging/discharging status of the BSS at representative day r and time t (1 = ON, 0 = OFF) [Binary]
$e_{r,t}^{BSS}$	Energy stored in the BSS at representative day r and time t [kWh]

1. Introduction

1.1. Context & motivation

Sustainable energy supplying of remote rural areas entails important techno-economic barriers. Frequently, deploying infrastructures for energy provision of these zones supposes unaffordable monetary expenditures occasioned for large investments and energy losses [1]. In this context, the Nanogrid (NG) and microgrid paradigms have

emerged as important frameworks to promote the penetration of renewable energies or provide reliable and continuous electricity service to isolated communities [2,3]. This fact is supported by various successful projects undertaken through the world such as the case of Gwagwalada-Abuja [4] and Sudan Savannah region, both in Nigeria [5]; or Jeju Island, in South Korea [3], among others.

The integration of renewable sources along the development of new energy exchange systems in multi-energy grids [6,7], has complicated the design stage of renewable-based systems. Proper sizing of a renewable hybrid system is a crucial task on deciding its feasibility, proper energy management [8–11] and enhancing reliability of energy supplying [12–14]. In isolated electrical systems, although the energy storage system is optional, it is generally present to add stability and ensure the balance between generation and demand. Furthermore, battery storage systems (BSSs) are recognized as the most appropriate for small-scale grids due to their size [15], reducing the cost of electricity by recharging in hours of low-cost periods and discharging during periods of high cost. In this context, those methodologies suitable for properly planning this kind of systems on NGs and microgrids become essential for operators and owners, as the optimal design of the BSS frequently determines the techno-economic viability of these grids. Despite this, most of available methodologies for BSS planning have several research gaps that can be improved from different points of view. This paper contributes to the pool of existing approaches for BSS planning in NGs and microgrids by proposing a novel methodology.

1.2. Literature review

The NG paradigm is relatively new. Several references define NG as a set of generators that supply small loads such as buildings or villages with powers between 0 - 100 kW [16]. Nevertheless, both NG and microgrid are frequently indistinguishable concepts. In

order to avoid any confusion, we have considered the both definitions in this Literature Review.

In the literature, the strategies of dimensioning, planning, operation and control of isolated grids have been widely investigated, combining different renewable sources, such as solar energy and biomass. The authors in [17], carry out an analysis of a hybrid renewable system for a rural population in India. The study focused on three different types of battery technologies, using nine metaheuristic algorithms in the Matlab® environment. The results indicate that the Salp Swarm algorithm results the most competitive algorithm for the concerned problem [18]. The study carried out in the reference [17] is not as comprehensive as a BSS planning tool requires. For instance, further results about different depth of discharge (DOD) settings were not provided and some conventional technologies such as Nickel-Cadmium (NiCd) and Sodium-Sulfur (NaS) were not contemplated in the analysis.

In [19], a comprehensive BSS sizing model for microgrid applications using Mixed-Integer linear programming is presented. The authors analysed different factors such as battery technology and DOD strategies were investigated. The developed tool offered acceptable results, however, some important indicators like variable operation and maintenance (O&M) and replacement costs are not included in the analysis. In addition, the developed analytic Mixed-Integer Linear Programming contemplates planning and operating horizon analysis on a whole, which supposes an unaffordable computational burden (various hours).

An energy and economic management of a microgrid considering different characteristics of the BSS is studied in [20]. In this paper, the impact of the DOD settings and the number of charge/discharge cycles of each BSS in the useful life of the grid is investigated. However, the authors did not study different time horizons, from planning

to operating conditions, which reduces the precision and practicality of the results obtained. In addition, the impact of some decisive factors on the final result, such as replacement costs, was overlooked.

The optimal planning of a microgrid or nanogrid which encompasses a BSS is normally posed as a Mixed-Integer linear (or even nonlinear) programming, which may pose serious difficulties on conventional software and tools. This issue has motivated to some authors to employ metaheuristic optimization techniques, which generally do not ensure the optimality of the results and are large time-consuming. Such is the case of the reference [21], in which the authors use different metaheuristic algorithms have been employed to determine the optimal sizing of a renewable system. Similarly, in [22] and [23] the authors used genetic algorithms for optimally planning different grid layouts with different battery technologies. On the other hand, a heuristic approach is considered in [24] for comparing two types of batteries (Lead-acid and Lithium-Ion (Li-ion)) in an isolated renewable system composed of solar panels and diesel generators. Along the drawbacks derived from the usage of heuristic approaches, these works present other gaps. For example, the paper [21] did not comprehensively compare different DOD settings while the studies [22–24] did not contemplate replacement and O&M costs, this way that the economic results cannot be properly analysed in the long term.

Other studies use specific software for optimally determine the grid layout. Such is the case of the software Hybrid Optimization Model for Multiple Energy Resources Professional (HOMER Pro®), which has been profusely used in recent years [25–27]. Although HOMER Pro® is a powerful tool for designing hybrid systems, it suffers of three main issues. 1) The amount of data that this software offers are limited, since it does not contemplate capital factors like the number of charging-discharging cycles completed through a year; this limitation is because HOMER Pro® design the system from a

planning time horizon, in that sense, some helpful results cannot be provided. 2) This software sizes the system from a deterministic point of view. Thus, the backup generator (e.g. Diesel Engine Generator (DEG)), is sized so that the peak demand can be fully covered by itself. In addition, the remainder components are assumed to work following a predetermined control strategy rather than based on an optimal scheduling program. 3) It does not contemplate important aspects like variable O&M expenditures or installation costs.

1.3. *Contributions & paper organization*

Clearly, the optimal design of a storage system for NG and microgrid applications has become a crucial work nowadays. This kind of studies are strongly influenced by the methodology considered for determining the capacities and optimal sizing of the grid layout, which has a direct impact in the profitability and reliability of the project.

This paper contributes to the pool of the different available methodologies for optimal planning of BSSs in NGs or microgrids by developing a novel methodology. Our proposal aims at overcoming some of the problems presented by other state-of-art methodologies as those indicated below:

- Generation and demand uncertainties are normally handle based on statistical analysis or complex approaches, which frequently ignores the particularity of the system under study or have a non-universal character.
- A comprehensive analysis of a BSS requires a large amount of results, which are obtained from different time horizon analyses. Most of available methodologies fail to manage with different time horizons from planning to operating conditions.
- Some costs associated with a BSS are frequently not contemplated.
- Many of available methodologies are computationally very expensive.

- Optimality of the results obtained is sometimes not guaranteed due to the application or heuristic or metaheuristic approaches.

To overcome the issues listed above, our proposal originally combines several approaches like clustering techniques, software and optimization tools. The developed framework is carried out in various stages, which cover different time horizons from planning to operation. This methodology is founded on the gaps showed by the different tools involved, which has motivated to combine various approaches in order to obtain the key benefits of each one. Thus, while the system layout is determined with the software HOMER Pro®, other key aspects of a BSS are determined by posing an optimal day-ahead scheduling tool in form of Mixed-Integer quadratic programming. Hence, the size of the system is determined on a planning horizon whereas other aspects like the project lifetime or different technologies evaluation are carried out by using analytic optimization techniques over a 1-year time horizon. Finally, a Net Present Value (NPV) analysis is carried out to analyse other associated costs over the project lifetime. Resulting methodology is quite effective and efficient and allows to comprehensively design a BSS providing a large amount of results and helpful data. For illustrative purposes, the designed methodology is applied to a prospective NG project in the region of Cuenca, Ecuador.

Remainder of this paper is organized as follows. Section 2 overviews the developed methodology and its foundations. Section 3 presents the mathematical formulation of the designed day-ahead optimal scheduling tool. Section 4 describes the illustrative case study used in simulations. Section 5 presents various results on the case study in order to show the capabilities of the developed methodology. Section 6 discusses several modifications of the proposed approach with the aim at providing further helpful capabilities. Finally, the main conclusions are duly drawn in Section 7.

2. Overview of the developed methodology

Instead of developing a universal technique that gathers all the desired requirements, in this paper it has been chosen to originally combining different tools which, separately, are strong in different tasks. BSS planning in NGs and microgrids may overcome different difficulties. For each arisen difficulty, a specific software, available technique or developed tool is used with the aim of effectively overcoming it. Consequently, the developed methodology would gather the strengths of the different tools and techniques involved. This way, an original multistage framework has been developed, which aims at taking advantage of the strengths of different applications. Fig. 1 displays a flowchart of the developed methodology for comprehensive planning a BSS for a NG or microgrid. The following sections are devoted on further explaining the developed methodology.

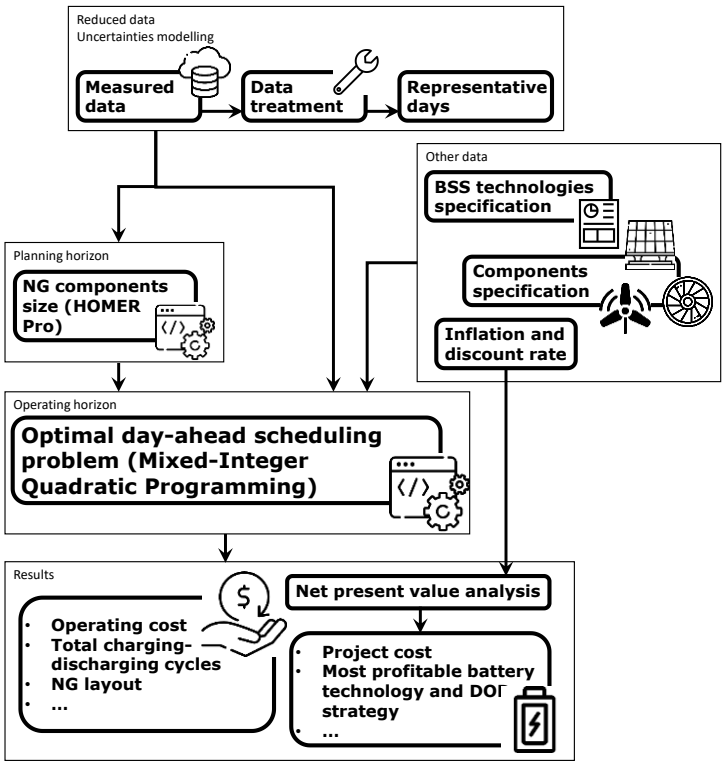

Figure 1. Flowchart of the proposed methodology

2.1. Data treatment and uncertainty handling

The developed tool assumes that any study parts from available raw data. Typically, solar irradiation, local demand, river speed or wind speed, are characteristic raw data for

this kind of analysis. All measured data is susceptible to contain inaccuracies and outliers, which are typically caused by untimely incidents, unexpected events, or device failures. Therefore, prior to any simulation or carrying out other stages, the available data should be properly treated. This issue can be effectively addressed by using filters [28].

On the other hand, planning studies typically cover large time horizons (from one year to decades). These prospective studies consequently span a huge amount of data which is also subjected to the highly variable, unpredictable, and location-specific characteristics of intermittent renewable energy sources. These facts frequently lead to computational intractability issues [29,30]. The uncertainty and large amount of data available is normally treated via scenarios, however, this approach entails important issues like difficulty to select the most suitable number of scenarios to consider and the probability of occurrence of each of them. In addition, traditional techniques like Monte Carlo requires generating a huge number of scenarios to obtain accurate results.

To overcome these issues above, a temporal representation based on a set of selecting representative days has been used [31]. It basically consists on clustering the available data for extracting the most representative profiles, which are considered an accurate representation of the whole measurements. This technique has been preferred over other traditional tools due to it presents three important advantages:

- This approach is not actually based on simply generating scenarios on the basis of some statistical principle rather than taking advantage of real measured data. Therefore, it can be concluded that the ‘scenarios’ used in simulations are in fact real profiles.
- The total number of representative days (scenarios) to consider can be easily setting by using helpful indexes [32]. Frequently, the total number of

representative days that should be considered for obtaining accurate results is much lower that the total number of scenarios required by other techniques.

- The probability of each representative day is immediately obtained from the total number of elements within each cluster.

In this paper, the k-medoids method has been used for obtaining the representative days of the available measurements. This technique usually offers an acceptable performance as pointed out in [33]. The k-medoids technique clusters the available data and identify the so-called medoids of each cluster. In practise, these medoids can be considered the representative days for our study. This methodology has a degree of freedom, namely the total number of clusters (i.e. the total number of representative days). Frequently, the total number of clusters (representative days), is selected based on heuristic criteria with the supporting of some helpful indicators like the Davies Bouldin index [32].

On the other hand, prior to BSS design, some auxiliary components data like batteries lifetime or O&M costs have to be provided as inputs for the algorithm.

2.2. Optimization over different time horizons

A tool for comprehensively planning BSSs should provide a large amount of results which are normally obtained over different time horizons. For example, the capacity of the storage system is frequently calculated over a planning time horizon, while other relevant aspects like the total charging-discharging cycles completed through a day should be determined over short-time horizons (e.g. hours-days). In this regard, different tools have been used for BSS design over planning and operating time horizons.

2.2.1. Planning horizon stage

A first approach to the optimal grid layout design is done by using the software HOMER Pro® [34]. This tool determines the optimal size of the different NG

components to fully supplied the yearly demand by own resources like Photovoltaic (PV) panels, backup units or wind generators.

2.2.2. Operating horizon stage

Although HOMER Pro® is a powerful tool for optimally design small-scale isolated grids, it presents several important issues (see Introduction). Therefore, we consider this software unable to comprehensive planning a BSS by itself. Hence, it is necessary to calculate some relevant results that HOMER Pro® is unable to provide. These results are contemplated over an operating time horizon of the system under study. To that end, a day-ahead optimal scheduling tool is developed. This framework solves the scheduling problem of the analyzed system in an analytic way as it is posed as a Mixed-Integer Quadratic programming (see Section 3).

From a computational point of view, this stage supposes the main bottleneck of the developed approach. One should note that this stage must be repeatedly solved for different parameters like DOD strategies or battery technology, which may suppose an unaffordable computational effort in some situations. However, this stage can be efficiently solving by using some advanced tools like Gurobi [35] or parallelization strategies (see Section 6).

2.3. Optimization variables

Because the developed methodology contemplates two optimization stages over different time horizons, each problem involves different variables. In order to clarify this point, Table 1 summarizes the variables involved each stage. It is worth noting that the variables considered in the planning horizon problem are taken as parameters in the operating horizon problem, therefore, these two tools have to be carried out sequentially.

Table 1. Variables involved in each optimization problem

Planning horizon problem	**Operating horizon problem**	
- Total PV capacity	$p_{r,t}^{PV}$	$p_{r,t}^{BSS,D}$
- Total WG capacity	$p_{r,t}^{WG}$	$\delta_{r,t}^{DEG}$
- Total HK capacity	$p_{r,t}^{HK}$	$\delta_{r,t}^{BSS,C}$
- Rated power of DEG	$p_{r,t}^{DEG}$	$\delta_{r,t}^{BSS,D}$
- BSS capacity	$p_{r,t}^{BSS,C}$	$e_{r,t}^{BSS}$

It is important to clarify that, in the planning optimization problem, the variables involved are the capacity or rated power of each component. However, since the rated power of some components is fixed by manufactures, the actually variables would be the number of components. Anyway, this aspect has not a significant importance and can be taken for convenience.

2.4. Final results provided

The results provided for the operating horizon optimization tool are referred to just one year. To extend the results obtained over the project lifetime and, consequently, properly determine the most suitable battery technology and DOD strategy, a NPV analysis is performed over the project lifetime. In this stage, the inflation and discount rate are introduced as parameters and other important aspects like the capital and replacement costs become crucial.

Lastly, the different stages involved within the developed methodology provide a large amount of relevant results. For the sake of summarizing, some of them (but not limited to), are summarized in the Table 2.

Table 2. Some relevant results provided by the developed methodology

Planning horizon problem	**Operating horizon problem**	**NPV analysis**
- Grid layout - Components size and capacity	- Yearly operating cost - Total charging-discharging cycles of BSS - Usage rate of each NG component - O&M costs analysis	- Project cost - Most suitable battery technology and DOD strategy - Payback period

3. Mathematical formulation of the day-ahead optimal scheduling problem

The following sections are devoted on describing the mathematical modelling of the developed day-ahead optimal scheduling problem involved within the developed methodology. It has been considered the different devices involved in the NG under study (see Section 4), however, similar principles can be applied to any other system configuration.

3.1. Modelling the PV system

For a PV array, the available power of the PV system as a function of the solar irradiance is given by [36].

$$\hat{p}_{r,t}^{PV} = 10^{-3} \cdot N^{PV} P^{PV} g^{PV} \left(\frac{I_{r,t}}{I_S}\right)\left[1 + \alpha^{PV}\left(T_{r,t}^{cell} - T_S\right)\right], \forall r \in \Psi_R, \forall t \in \Psi_T, [\text{kW}] \qquad (1)$$

where

- N^{PV} is the number of panels of the PV array.
- P^{PV} is the rated power of a PV panel.
- g^{PV} is derating factor of the PV array.
- $T_{r,t}^{cell}$ is cell temperature at representative day r and time t.
- T_S is the temperature under standard conditions (25 ºC).
- Ψ_R is the set of representative days.
- Ψ_T is the set of time intervals within the studied time horizon.

In (1), the so-called cell temperature ($T_{r,t}^{cell}$) is calculated for each representative day and time, as follows.

$$T_{r,t}^{cell} = T_{r,t} + I_{r,t}\left[\frac{T_{NOCT}^{C} - T_{NOCT}^{A}}{I_{NOCT}^{T}} \times \left(1 - \frac{\eta^{PV}}{0.9}\right)\right], \forall r \in \Psi_R, \forall t \in \Psi_T \quad (2)$$

where

- $T_{r,t}$ is the temperature at representative day r and time t.
- $I_{r,t}$ is the solar irradiance at representative day r and time t.
- η^{PV} is the solar panel efficiency.

The energy produced by the renewable-based units is limited by the availability of natural resources. In the case of the PV array, the amount of solar irradiation determines the power given by the PV unit by the equation (1). So that, this kind of units cannot be categorized as dispatchable. Nevertheless, the power given by the PV system can be still lower than $\hat{p}_{r,t}^{PV}$ if required. Thus, the following constraint must be satisfied.

$$p_{r,t}^{PV} \leq \hat{p}_{r,t}^{PV}, \forall r \in \Psi_R, \forall t \in \Psi_T \quad (3)$$

The O&M variable costs of the PV system are proportional to the energy generated by this unit [20], as follows.

$$f_{r,t}^{PV} = \Delta\tau a^{PV} p_{r,t}^{PV}, \forall r \in \Psi_R, \forall t \in \Psi_T \quad (4)$$

where

- a^{PV} are the O&M variable costs of the PV system.

3.2. Modelling the wind generation system

Normally, the available data is provided in form of wind speed, which should be converted to power units by using the well-known speed-power curve of the wind turbine. This relationship is normally nonlinear, so, a piecewise equivalence is frequently adopted [20,36]. The operation of a wind turbine is limited between two characteristics wind speeds called cut-in and cut-off. When the available wind speed is out of the range defined by these parameters, the wind turbine is not operated. Thus, the available power of a Wind Generator (WG) system can be expressed as

$$\hat{p}_{r,t}^{WG} = 10^{-3} \cdot N^{WG} A^{WG} \rho^{W} \eta^{WG} \times$$

$$\begin{cases} 0, \text{for } V_{r,t}^{W} < V^{WG,cut-in} \\ \alpha^{WT} V_{r,t}^{W\,3} - \beta^{WG} P^{WG}, \text{for } V^{WG,cut-in} < V_{r,t}^{W} < V^{WG} \\ P^{WT}, \text{for } V^{WG} < V_{r,t}^{W} < V^{WG,cut-out} \\ 0, \text{for } V_{r,t}^{W} > V^{WG,cut-out} \end{cases}, \forall r \in \Psi_R, \forall t \in \Psi_T, [\text{kW}] \qquad (5)$$

where

- N^{WG} is the number of wind turbines of the WG system.
- A^{WG} is the Turbine swept area of the WG system.
- ρ^{W} is the air density.
- η^{WG} is the efficiency of the WG system.
- $V^{WG,cut-in}/V^{WG,cut-out}$ is the cut-in/cut-out speed of the WG system.
- P^{WG} is the WG output electric power.

In (5), the coefficients α^{WG} and β^{WG} are coefficients calculated as follows.

$$\alpha^{WG} = \frac{P^{WG}}{V^{WG\,3} - V^{WG,cut-in\,3}} \qquad (6)$$

$$\beta^{WG} = \frac{V^{WG,cut-in\,3}}{V^{WG\,3} - V^{WG,cut-in\,3}} \qquad (7)$$

As for the PV system, the value calculated in (5) supposes an upper bound for the power given by the WG at time t and representative day r, as follows.

$$p_{r,t}^{WG} \leq \hat{p}_{r,t}^{WG}, \forall r \in \Psi_R, \forall t \in \Psi_T \quad (8)$$

Similar to the PV system, the O&M variable costs of the WG system is a linear function of the energy produced, as follows.

$$f_{r,t}^{WG} = \Delta\tau a^{WG} p_{r,t}^{WG}, \forall r \in \Psi_R, \forall t \in \Psi_T \quad (9)$$

where

- a^{WG} are the O&M variable costs of the WG system.

3.3. Modelling the Hydrokinetic system

The available power of a Hydrokinetic (HK) system can be modelled similarly to the WG system [37]. Thus, the power given by this unit is normally bounded by characteristics maximum and minimum river speeds. Consequently, the available power of the HK system is given by.

$$\hat{p}_{r,t}^{HK} = 10^{-3} \cdot N^{HK} A^{HK} C_p \rho^{H_2O} \eta^{HK} \times$$

$$\begin{cases} 0, \text{for } V_{r,t}^{RV} < V^{HK,cut-in} \\ \frac{V_{r,t}^{RV\,3}}{2}, \text{for } V^{HK,cut-in} < V_{r,t}^{RV} < V^{HK,cut-out} \\ 0, \text{for } V_{r,t}^{RV} > V^{HK,cut-out} \end{cases}, \forall r \in \Psi_R, \forall t \in \Psi_T, [\text{kW}] \quad (10)$$

where:

- N^{HK} is the number of turbines of the HK system.
- A^{HK} is the turbine swept area of the HK system.
- ρ^{H_2O} is the water density
- C_p Power coefficient of a turbine performance.

- η^{HK} is the efficiency of the HK system.
- $V^{HK,cut-in}/V^{HK,cut-out}$ is the cut-in/cut-out speed of the HK system.

As the others renewable-based units, the power given by the HK system is upper limited by the value calculated in (10). Hence, the following constraint must be satisfied.

$$p_{r,t}^{HK} \leq \hat{p}_{r,t}^{HK}, \forall r \in \Psi_R, \forall t \in \Psi_T \quad (11)$$

Similar to the PV and WG systems, the O&M variable costs of the HK systems are a function of the energy exchanged with the NG, as follows.

$$f_{r,t}^{HK} = \Delta\tau a^{HK} p_{r,t}^{HK}, \forall r \in \Psi_R, \forall t \in \Psi_T \quad (12)$$

where:

- a^{HK} are the O&M variable costs of the WG system.

3.4. Modelling the DEG

The power given by the DEG must be upper and lower bounded by operational limits. This restriction can be modelled as follows.

$$\delta_{r,t}^{DEG} p^{DG,min} \leq p_{r,t}^{DEG} \leq \delta_{r,t}^{DEG} p^{DEG,max}, \forall r \in \Psi_R, \forall t \in \Psi_T \quad (13)$$

where

- $\delta_{r,t}^{DEG}$ is the operation status of the DEG at representative day r and time t (1 = ON, 0 = OFF).
- $p^{DEG,min}/p^{DEG,max}$ min./max. capacity of the DEG.
- $p_{r,t}^{DEG}$ power given by the DEG system at representative day r and time t.

Also, the power given by the DEG between two consecutive time intervals cannot violate the so-called ramp-restrictions, as follows.

$$p_{r,t-1}^{DEG} - RD^{DEG} \leq p_{r,t}^{DEG} \leq p_{r,t-1}^{DEG} + RU^{DEG}, \forall r \in \Psi_R,\ \forall t \in \Psi_T / t > 1 \quad (14)$$

where

- $p_{r,t-1}^{DEG}$ is the power given by the DEG system at representative day r and time $t-1$.
- RD^{DEG}/RU^{DEG} Ramp down/up limits of the DEG.

Unlike to the renewable-based units, the DEG works as a fuel-fired generator. So, their operation costs are strongly influenced by the fuel cost. The fuel costs of a DEG are typically modelled as a quadratic function of the power given by the DEG [38]. Also, an independent may be included to model the fixed costs by unit of time. Thus, the fuel and O&M variable costs of the DEG will be given by.

$$f_{r,t}^{DEG,op} = a^{DEG}\Delta\tau\delta_{r,t}^{DEG} + b^{DEG}P_{r,t}^{DEG} + c^{DEG}{P_{r,t}^{DEG}}^2, \forall r \in \Psi_R, \forall t \in \Psi_T \quad (15)$$

where

- $\delta_{r,t}^{DEG}$ is the operation status of the DEG at representative day r and time t.
- $a^{DEG}, b^{DEG}, c^{DEG}$ are cost coefficients of the DEG.

Also, the start-up and shutdown costs should be included as follows.

$$f_{r,t}^{DEG,su+sd} = \lambda^{DEG}\max\left(0, \left|\delta_{r,t}^{DEG} - \delta_{r,t-1}^{DEG}\right|\right), \forall r \in \Psi_R, \forall t \in \Psi_T > 1 \quad (16)$$

where

- λ^{DEG} are the startup/shutdown costs of the DEG.

So, the total operating costs will be the combination of the O&M, fuel, start-up, and shutdown costs, as follows.

$$f_{r,t}^{DEG} = f_{r,t}^{DEG,op} + f_{r,t}^{DEG,su+sd}, \forall r \in \Psi_R, \forall t \in \Psi_T \quad (17)$$

3.5. Modelling the BSS

The rated power of the BSS is limited by its capacity and the so-called energy-to-power ratio. The charging and discharging power of a BSS system is, consequently, limited by the constraints (18) and (19). The equation (20) models the state of charge of the BSS at time t. The capacity of the BSS is always upper limited by its capacity and lower limited by the selected DOD value, as says the equation (21). In this paper, we have considered that the initial energy stored in the BSS is unknown. Thus, it is modelled by a random number ν which is generated by a truncated Gaussian distribution with mean 1, standard deviation 0.1 and limits 0.95-1. This way, according to (22), the initial state of charge each representative day may vary around S^{BSS}; on the other hand, the state of charge of the BSS at the end of each representative day can also vary around S^{BSS}, however, the equation (23) forces it to be always higher than a 95% of the total capacity of the storage system by security reasons. In addition, this aspect is also penalized in the objective function (see eq. (28)). Finally, the charging and discharging processes of the BSS are complementary, as modelled the equation (24).

$$0 \leq p_{r,t}^{BSS,C} \leq \delta_{r,t}^{BSS,C} \frac{S^{BSS}}{E2P^{BSS}}, \forall r \in \Psi_R, \forall t \in \Psi_T \tag{18}$$

$$0 \leq p_{r,t}^{BSS,D} \leq \delta_{r,t}^{BSS,D} \frac{S^{BSS}}{E2P^{BSS}}, \forall r \in \Psi_R, \forall t \in \Psi_T \tag{19}$$

$$e_{r,t}^{BSS} = e_{r,t-1}^{BSS} + \left(\eta^{BSS,C} p_{r,t}^{BSS,C} - \frac{p_{r,t}^{BSS,D}}{\eta^{BSS,D}}\right) \Delta\tau, \forall r \in \Psi_R, \ \forall t \in \Psi_T / t > 1 \tag{20}$$

$$(1 - DOD^{BSS}) S^{BSS} \leq e_{r,t}^{BSS} \leq S^{BSS}, \forall r \in \Psi_R, \forall t \in \Psi_T \tag{21}$$

$$e_{r,1}^{BSS} = \nu S^{BSS}, \forall r \in \Psi_R \tag{22}$$

$$e_{r,T}^{BSS} \geq 0.95 \cdot S^{BSS}, \forall r \in \Psi_R \tag{23}$$

$$\delta_{r,t}^{BSS,C} + \delta_{r,t}^{BSS,D} \leq 1, \forall r \in \Psi_R, \forall t \in \Psi_T \quad (24)$$

where

- $p_{r,t}^{BSS,C}/p_{r,t}^{BSS,D}$ is the charging/discharging power of the BSS at representative day r and time t.
- S^{BSS} is the capacity of the BSS.
- $E2P^{BSS}$ is the Energy-to-power ratio of the BSS system.
- $e_{r,t}^{BSS}$ is the energy stored in the BSS at representative day r and time t.
- $\eta^{BSS,C}/\eta^{BSS,D}$ is the charging/discharging efficiency of the BSS system.
- DOD^{BSS} depth of discharge of the BSS system.
- ν is a random number generated by a truncated Gaussian distribution with mean 1, standard deviation 0.1 and limits 0.95-1.

The O&M variable costs of a BSS are normally proportional to the total energy exchanged with the NG [19]. Similarly, to the renewable-based units, these costs can be calculated as follows.

$$f_{r,t}^{BSS} = \Delta\tau a^{BSS}\left(p_{r,t}^{BSS,C} + p_{r,t}^{BSS,D}\right) \quad (25)$$

where:

- a^{BSS} are the O&M variable costs of the BSS.

On the other hand, the lifetime of a BSS is strongly influenced by the total number of charging-discharging cycles. This value through a year can be calculated by using the developed day-ahead optimal scheduling model, as follows.

$$Cycles_{year} = \sum_{\Psi_R} \frac{\Delta\tau\rho_r}{2S^{BSS}}\left(\sum_{\Psi_T}\left(p_{r,t}^{BSS,C} + p_{r,t}^{BSS,D}\right)\right) \quad (26)$$

The equation (26) compares the energy exchanged between the grid and the BSS with the total capacity of batteries, thus, the total daily charging-discharging cycles are calculated for each representative day. To extend the results obtained to one-year time horizon, each daily result is weighted by the total number of representative days within each cluster (ρ_r).

3.6. Grid balance

The system under study will be sized so that the total peak demand can be fully covered by the backup generator (e.g. a DEG). Therefore, the demand can be fully satisfied through a year and, consequently, the constraint (27) must be satisfied.

$$p_{r,t}^{PV} + p_{r,t}^{WG} + p_{r,t}^{HK} + p_{r,t}^{BSS,D} + p_{r,t}^{DEG} = p_{r,t}^{Demand} + p_{r,t}^{BSS,C}, \forall r \in \Psi_R, \forall t \in \Psi_T \quad (27)$$

3.7. Objective function

In this case, we pose an objective function from the NG operator/owner, so that the fully demand is satisfied at minimum cost. This way, the objective function encompasses the operational costs of the different units deployed through the study system and a penalty function which aims at encouraging that the BSS is fully charged at the end of each day. More precisely, the objective function for the designed optimization problem is defined as follows.

$$\min_{\Phi} \sum_{\Psi_R} \left\{ \rho_r \left[\gamma \left(\frac{S^{BSS} - e_{r,T}^{BSS}}{0.95 \cdot S^{BSS}} \right) + \sum_{\Psi_T} \left(f_{r,t}^{DEG} + f_{r,t}^{PV} + f_{r,t}^{WG} + f_{r,t}^{HK} + f_{r,t}^{BSS} \right) \right] \right\} \quad (28)$$

where Φ is the vector of decision variables given by.

$$\Phi = \{ p_{r,t}^{PV}, \forall r \in \Psi_R, \forall t \in \Psi_T; p_{r,t}^{WG}, \forall r \in \Psi_R, \forall t \in \Psi_T; p_{r,t}^{HK}, \forall r \in \Psi_R, \forall t \in \Psi_T; p_{r,t}^{DEG}, \delta_{r,t}^{DEG}, \forall r \in \Psi_R, \forall t \in \Psi_T; p_{r,t}^{BSS,C}, \delta_{r,t}^{BSS,C}, \forall r \in \Psi_R, \forall t \in \Psi_T; p_{r,t}^{BSS,D}, \delta_{r,t}^{BSS,D}, \forall r \in \Psi_R, \forall t \in \Psi_T; e_{r,t}^{BSS}, \forall r \in \Psi_R, \forall t \in \Psi_T \} \quad (29)$$

In (28) the f's represent the operation costs of the different units deployed through the study NG; while the penalty term considers that the NG operator desires to get the BSS fully charged at the end of each day, consequently, any other state of charge is penalized. The developed day-ahead optimal scheduling problem is Mixed-Integer Quadratic Programming, which has been coded in Matlab R2019a and solved by using Gurobi [35].

4. Overview of the illustrative case study: a NG at Cuenca, Ecuador

In order to show the capabilities of the developed methodology as providing proper guidelines for its universal applicability, a prospective isolated system in the region of Cuenca, Ecuador has been considered as benchmark case study. This case is considered generic enough to serve as illustrative example. In that sense, the developed methodology could be applied to any other system in the same manner as it has been applied to this particular case. The considered case study is overviewed through this section.

In recent years, NG are increasingly studied, especially in developing regions, such as the case of the Cuenca, Ecuador area. This area includes several residential communities with a maximum demand of ~ 38 kW (2018), which are difficult to supply through the electrical distribution grid due to losses and high costs in transmission lines. Therefore, an isolated NG is being planned so that the inhabitants can supply with their own resources, taking advantage of the existence of promising renewable resources such as solar radiation, wind speed, and hydraulic resources. This has motivated several studies aimed at the design of an isolated alternating current (AC) NG scheme [39]. Since, key aspects such as profitability, technical viability or the life cycle of the project [19,40], have not been accurately determined yet, we consider this case an acceptable benchmark to apply the developed methodology. Real demand values have been measured for a community near Cuenca in Ecuador. The area under study is shown in Fig 2.

Figure 2. Community under study

The loads are mainly resistive and inductive, such as lighting, household appliances and water heating. Although local demand does not exhibit a clear pattern, the peak load is often observed at 7:00 pm, as shown in Fig. 3, with a maximum of approximately 33 kW and the valley demand in the early morning with around 20 kW.

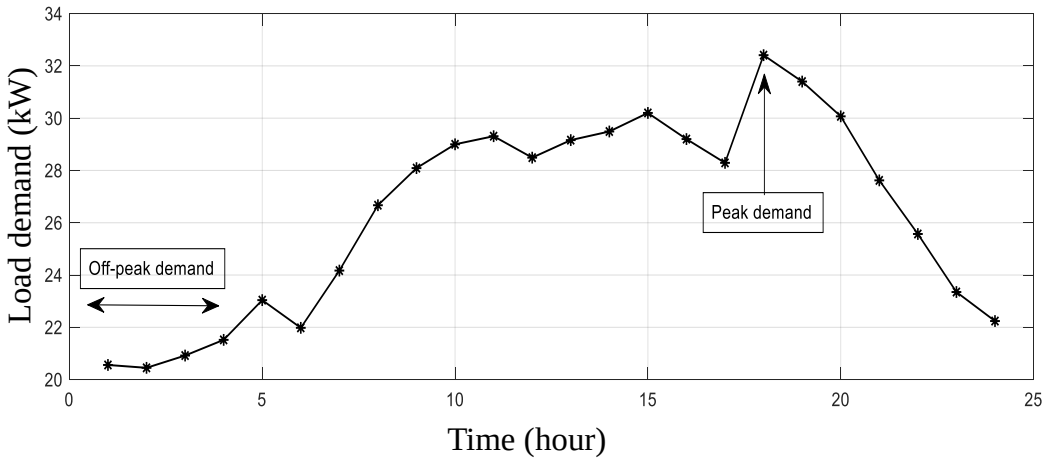

Figure 3. Typical daily load curve, [kW]

However, the average monthly peak demand is around 25.6 kW and occurs during the months of April and December, and the average monthly off-peak demand is around 23.7 kW during the months of July and August as shown in Fig 4. The seasonal variation is caused mainly by vacation times when the inhabitants usually leave the community.

Average monthly renewable resources are shown in Fig. 4, water speed and solar radiation show an increasing trend from July onwards, with maximum monthly hourly

averages of 4 m/s and 6 kW/m^2 respectively, while the wind speed has an inverse behaviour and has a maximum monthly hourly average of 5.5 m/s.

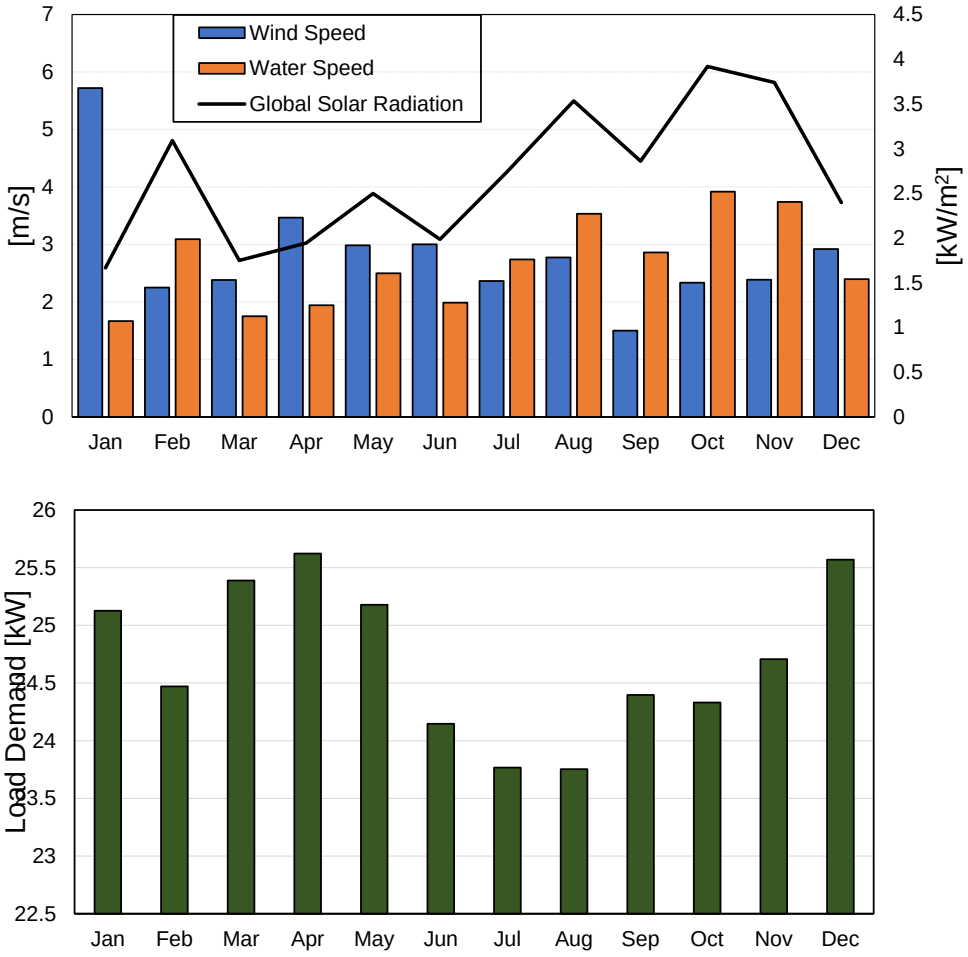

Figure 4. Renewable resources in the study area (upper); and load demand represented by average monthly and hourly values (bottom)

The main characteristics of the renewable energy sources used in this study located in the NG laboratory of the University of Cuenca are shown in Table 3 and Fig. 5.

Figure. 5 Renewable energy sources available in the NG laboratory

Table 3 Parameters of renewable energy sources

Data of PV Panels [41]	
Rated power	250 W
Panel surface	1.63 m²
Efficiency	16.70%
Data of WG [41]	
Rated power	5,500 W
Inverter MPPT + WG efficiency	48.50%
Swept area	14.52 m²
Cut-in spped	2 m/s
Rated speed	11 m/s
Cut-out speed	21 m/s
Data of HKs [41]	
Rated power	5,000 W
Efficiency	50%
Swept area	0.785 m²
Cut-in speed	1 m/s
Cut-out speed	3.1 m/s

Five different profiles are of interest for the present study; wind speed, solar irradiance and temperature data have been extracted from a meteorological station located near the study area, with time periods of one hour during 2018 [41]. The water speed has been calculated from data of flows and daily river levels for a year, taken from the meteorological station H0894 [42]. Furthermore, smart energy meters have been used to record electrical demand values for one year in kWh.

5. Numerical Results

5.1. Data treatment and representative days

The available measured data has been previously filtered by using a 6-hour moving average filter [28] to remove bad data and outliers. This kind of filter has the effect of smoothed the measured curves and, consequently, reducing the noise introduced by bad data and outliers.

Once the measured data has been properly treated, it is suitable to characterize it by means of representative days. As commented, the k-medoids technique has been used in this paper due to their good features. This technique presents a degree of freedom namely the total number of clusters (i.e. representative days), which is a parameter that has been set by the user. However, one can use some helpful indexes for supporting this decision. In this case, the total number of representative days has been selected attending to two indexes namely the total sum of distances, which reflects the sum of the distances between the medoid of each cluster with respect to the other members within it; and the Davie Bouldin index. Intuitively, one shall to reduce both indexes as much as possible, however, a trade-off between accuracy and computational burden is pursued. Fig. 6 plots the value of the two considered indexes for the system under study. As seen, selecting 10 representative days seems a good choice due to the total sum of distances is nor further reduced beyond it and the Davies Bouldin index is reasonably low for this clustering number. Fig. 7 plots the profiles of the selected 10 representative days.

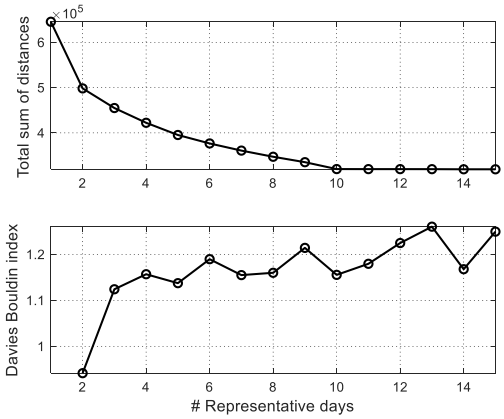

Figure 6. The value of the two helpful indexes used for evaluating the total number of representative days used in simulations. The total sum of distances (upper) and the Davies Bouldin index (bottom)

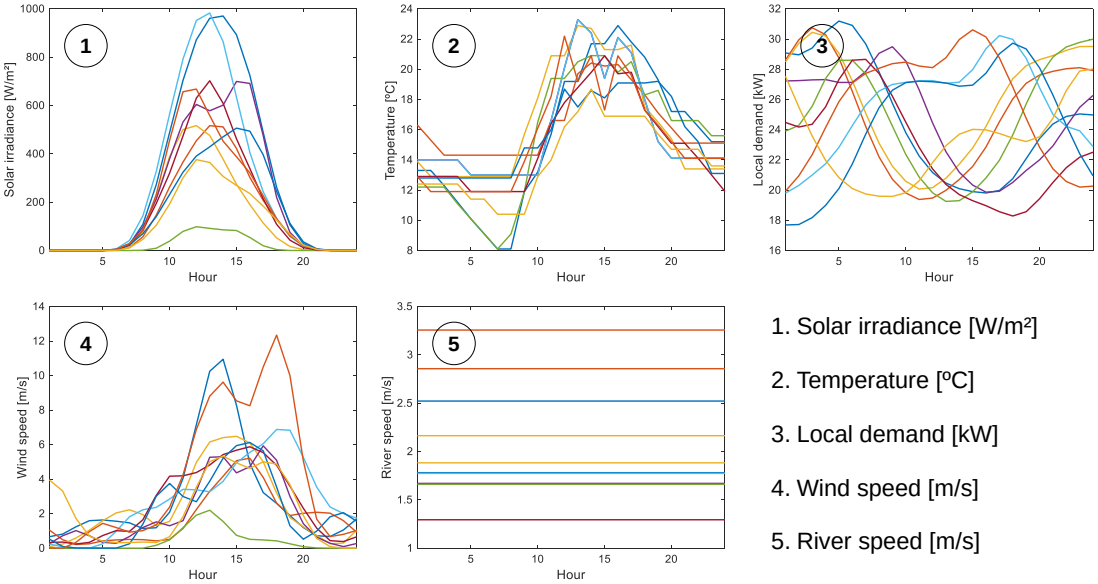

Figure 7. The profiles of the 10 representative days used in simulations

In Fig. 7, the local demand profile, it is observed that during certain days the demand peak occurs at dawn. This is due to the work routines of the inhabitants of the community and holidays. On the other hand, the speed of river during a day is constant. This behaviour is the result of the type of data measurement by the hydrological station in the site, which collects the river speed in daily average values (m/s/day). As 1-hour resolution is required (see Section 5.3), the available raw data has been interpolated over the study time horizon.

5.2. Components sizing (planning horizon)

The optimal size of the NG has been calculated using the HOMER Pro® software, which, using historical data based on the hourly input variables for one year (temperature, solar radiation, wind speed, water speed, demand), calculates the capacity of the sources and the energy storage system [34]. HOMER Pro® uses mathematical models to simulate the hybrid system minimizing the cost of energy, the results can be hundreds or thousands of similar simulations from which the most feasibility profitable is chosen [36]. In the objective function, the variables are battery capacity and DEG penetration, and the optimized powers from renewable sources are projected values. Energy management is chosen between three types of energy control, charge cycle load following and combined dispatch. In the first control, if the energy from renewable sources is insufficient to supply the demand and the batteries are discharged (that is, its state of charge is less than the minimum), the DEG starts at full load supplying the demand, and the remaining power is used to recharge the batteries. In the second control in case of not having enough energy from renewable sources considering that the batteries are discharged (the state of charge is less than the minimum value), the DEG only starts with the power required by demand at all times, without recharging the batteries. The combined dispatch chooses between the two previous controls depending on the energy cost in each time interval. In this case, the load following control turned out to be optimal. The BSS capacity has been calculated to cover all the electrical demand, reducing the CO_2 emissions.

The studied NG was simulated, for four different battery technologies: Lead-Acid, Li-ion, NiCd and NaS. The results obtained are summarized in Table 4. As seen, HOMER Pro® yielded different results depending on the BSS technology. In order to properly compare the different technologies, it is suitable to carry out this analysis for comparable systems, i.e. the same capacity of the BSS. In this paper, the comparative analysis of the

different technologies has been carried out taking the results obtained for the Li-ion technology. This has been done so since HOMER Pro® sizes the DEG so the peak demand can be fully covered by this device, this way the total yearly demand could be even covered without BSS. Therefore, continuity supplying is guaranteed regardless the battery technology. Thus, the BSS would be deployed with the end of reducing the dependency with the DEG, thus, the most profitable selection would be, a priori, a BSS capacity of 110 kWh since this value will reduce the capital and installation costs of the BSS as the total energy generated by the DEG is reduced.

Table 4. Summary of the results obtained with HOMER Pro® for different BSS technologies

Parameter	**Optimizer Method**	**Lead-Acid**	**Li-Ion**	**NiCd**	**NaS**
PV	Homer Optimizer	58 kW	53 kW	57 kW	56 kW
WG	1, 2, 3, 4, 5, 10, 15, 20 units	5.5 kW	5.5 kW	5.5 kW	5.5 kW
HK	1, 2, 3, 4, 5, 10, 15, 20 units	25 kW	25 kW	15 kW	15 kW
DEG	Homer Optimizer	40 kW	40 kW	40 kW	40 kW
BSS	Homer Optimizer	180 kWh	110 kWh	130 kWh	150 kWh

5.3. Different BSS technologies comparison (operating horizon and NPV analysis)

In this section, several simulations are carried out in order to analyse the suitability of different BSS technologies for the NG under study. Four battery technologies are considered: Lead-acid, NiCd, Li-ion and NaS, with different DOD values. The results are obtained by using the developed day-ahead optimal scheduling model described in the Section 3. This problem will be solved with a 1-hour time resolution ($\Delta\tau = 1$) over a 24 hours horizon ($T = 24$). Table 5 reports the cost coefficients of the different units, which have been extracted from [20,43–45]. As commented, the capacities of the different NG units were taken from the results obtained with HOMER Pro® by using Li-ion batteries

(see Table 4). Table 6 indicates the value of the parameter ρ_r for the different representative days. The minimum dispatchable power for the DEG will be 5kW, while their ramps constraints have been neglected for the case study since it is assumed that the DEG is able to schedule its total capacity in a time interval (1 hour). The energy-to-power ratio for the BSS is assumed to be 4 hours [46], while the efficiency of the considered BSS technologies are reported in Table 7 [19]. Finally, the penalty term γ has been taken equal to 10^3 \$, assuming that the BSS is only allowed to be partially charged at the end of each day in cases of few renewable generation or similar.

Table 5. Cost data of the different units

Unit		a	b	c	λ
DEG		0.6 \$/h	0.05 \$/kW	0.02 \$/kW²	*
PV		0.19 \$/kWh	--	--	--
WG		0.24 \$/kWh	--	--	--
HK		0.31 \$/kWh	--	--	--
BSS	Lead-acid	0.41 \$/MWh	--	--	--
	NiCd	--	--	--	
	Li-ion	2.35 \$/MWh	--	--	
	NaS	2.02 \$/MWh	--	--	

* The start-up and shutdown costs of the DEG are considered marginal for the calculated capacity

Table 6. The values of the different ρ_r's

$\rho_1 = 28$	$\rho_3 = 39$	$\rho_5 = 53$	$\rho_7 = 41$	$\rho_9 = 14$
$\rho_2 = 34$	$\rho_4 = 52$	$\rho_6 = 37$	$\rho_8 = 38$	$\rho_{10} = 29$

Table 7. Efficiencies for different Battery Technologies

Technology	$\eta^{BES,C}$	$\eta^{BES,D}$
Lead-acid	0.7	0.7
NiCd	0.8	0.8
Li-ion	0.98	0.98
NaS	0.95	0.95

As commented, to evaluate the performance of different BSS technologies and DOD strategies, it is primordial to properly model the behaviour of the BSS; more precisely, an accurate representation of the state of charge of the BSS is crucial. In this regard, the developed scheduling tool worked acceptably well. As seen in Fig. 8, the state of charge

of the BSS is proportional to the energy exchanged with the NG. Also, the maximum and minimum capacity of the BSS depends on the DOD strategy adopted, as shown in Fig. 9.

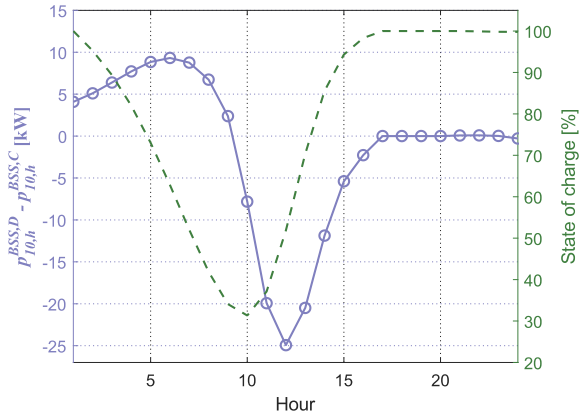

Figure 8. State of charge and delivered power from/to BSS to/from NG ($r = 10$, NiCd, DOD = 70%, $\gamma = 10^3$ and $\nu = 1$)

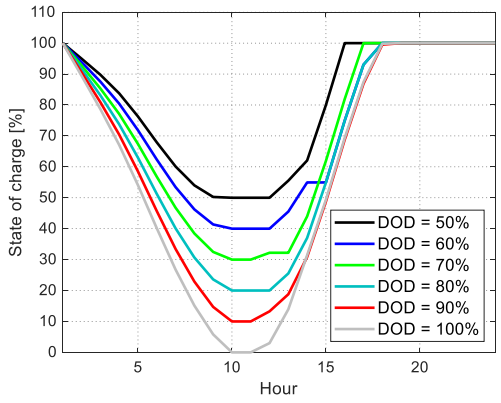

Figure 9. State of charge cycle for different DOD values ($r = 3$, NiCd, $\gamma = 10^3$ and $\nu = 1$)

Figure 10 shows a comparison of the daily operating cost with different battery technologies and DOD values. The scenario without battery facilities (base case), is also showed for comparison. As observed, the usage of BSS enables savings of ~30 $/day. More precisely, higher savings are achieved as deeper DOD are allowed, which was expected since by adopting this strategy the BSS is further exploited. The daily operating cost does not notably vary by using different technologies and mainly depend on the O&M costs of each technology. Thus, the cheapest operating conditions of the NG under study were achieved by using NiCd batteries (~17% reduction w.r.t. the base case).

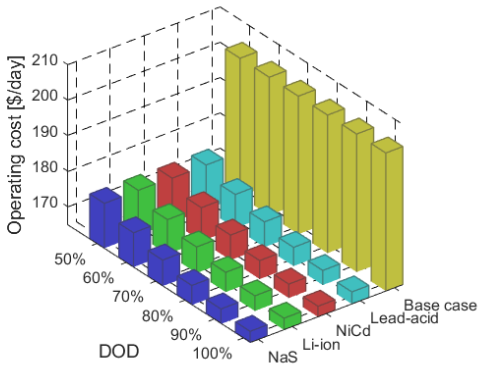

DOD [%]	Base case	Technology			
		Lead-Acid	NiCd	Li-ion	NaS
50	203.89	177.46	177.41	177.66	177.63
60	203.89	174.51	174.43	174.73	174.68
70	203.89	172.11	172.05	172.36	172.32
80	203.89	170.28	170.19	170.55	170.51
90	203.89	169.11	168.90	169.27	169.23
100	203.89	168.40	168.01	168.31	168.25

Figure 10. Operating daily cost [$/day] with different technologies and DOD values

Figure 11 shows the total energy produced by the DEG through a year. As expected, the total energy supplied by the DEG is proportional to the daily operating cost, which evidences that the usage of the DEG is only justify as backup generator, in the case of no availability of renewable-based units. In this case, the DEG generation is reduced regardless the battery technology considered. This is logic since tis value only depends on the energy exchanged between the grid and the BSS, which allows to reduce the dependency with the DEG. More precisely, the usage of a BSS allows to reduce the DEG generation by 14% through a year.

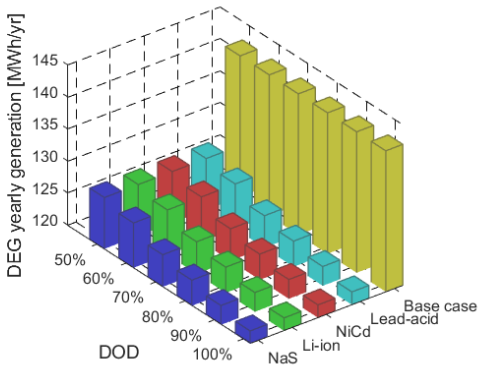

DOD [%]	Base case	Technology			
		Lead-Acid	NiCd	Li-ion	NaS
50	142	128	128	128	128
60	142	127	127	127	127
70	142	125	125	125	125
80	142	124	124	124	124
90	142	123	123	123	123
100	142	122	122	122	122

Figure 11. Energy generated by the DEG through a year [MWh/yr] with technologies and DOD values

The lifetime of a BSS is mainly determined by the calendric and cycling aging [19]. The former affects even if the BSS is not used while the latter is greatly influenced by the DOD and the total number of charging-discharging cycles. Thus, the lifetime of a BSS

technology is determined by either the calendric or cycling aging. Table 8 shows the expected lifetimes of different BSS technologies because calendric aging [45]. As seen, attending to this kind of battery degradation, the NiCd and NaS seem the most attractive solutions due to their longer lifetime. However, the cycling aging has to be also considered. In this regard, the developed scheduling tool allows an accurate representation of the charging-discharging cycles, so that, the lifetime of the BSS because cycling aging can be estimated. The total number of charging-discharging cycles completed for each storage technology with different DOD values through a year is plotted in Fig. 12. As expected, more cycles are completed as deeper DODs are allowed. The total number of charging-discharging cycles completed through a year also depends on the efficiency of each technology. This was expected since those technologies with low efficiency require to exchange more energy with the system. Thus, the Lead-Acid batteries completed more cycles than the other technologies.

Table 8. Expected lifetimes due to calendric aging of different BSS technologies [45].

BSS technology	Expected Lifetime [yrs]
Lead-acid	5
NiCd	10
Li-ion	5
NaS	10

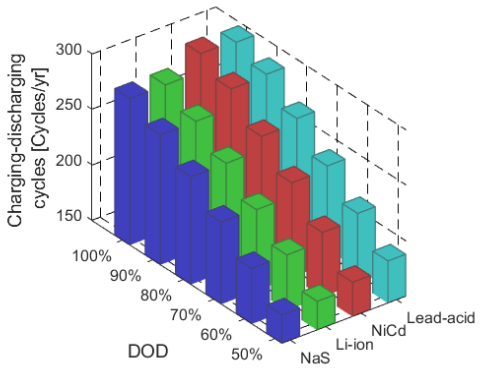

DOD [%]	Technology			
	Lead-Acid	NiCd	Li-ion	NaS
50	188	182	176	176
60	214	208	201	201
70	238	235	223	224
80	263	260	248	248
90	286	284	268	268
100	296	298	282	282

Figure 12. Total charging-discharging cycles through a year with different technologies and DOD values

Once the total number of charging-discharging cycles has been calculated, it is possible to estimate the lifetime of the considered technologies due to cycling aging. Typically, the lifetime of a BSS because cycling aging is given by a nonlinear relationship between the total charging-discharging cycles and DOD value. However, a piecewise approximation may be used [19]. In this regard, the expected lifecycles for each technology and DOD value are reported in Table 9 [19,20]. As seen, NaS batteries present the longest lifecycle while the Lead-acid technology allows very few charging-discharging cycles through its lifetime. Fig. 13 shows the expected lifetimes due to cycling aging for the considered storage technologies with different DOD values. As expected, the expected lifetime because cycling aging decreases as the DOD grows since more cycles tend to be completed. As observed, the Lead-acid and NiCd technologies show very short lifetime (~1-4 years). On the other hand, Li-ion and NaS batteries present large lifetimes when large DOD are not allowed (~20-50 years).

Table 9. Lifecycles for Various DOD Values and BSS technologies [19,33]

DOD	**Technology**			
[%]	**Lead-acid**	**NiCd**	**Li-ion**	**NaS**
50	700	1200	8000	10000
60	590	900	6900	9000
70	500	800	5800	7000
80	450	700	4500	6000
90	390	600	3700	5000
100	350	500	3000	4000

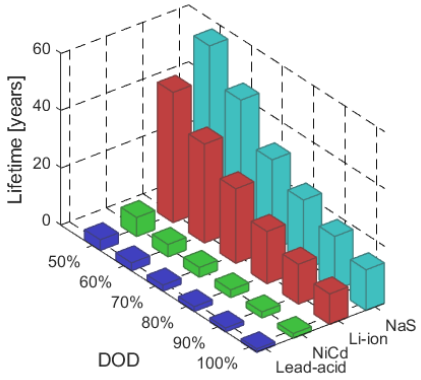

DOD [%]	Technology			
	Lead-Acid	NiCd	Li-ion	NaS
50	3.7	6.6	45.5	56.8
60	2.8	4.3	34.3	44.8
70	2.1	3.4	26.0	31.3
80	1.7	2.7	18.1	24.2
90	1.4	2.1	13.8	18.7
100	1.2	1.7	10.6	14.2

Figure 13. Expected lifetimes due to cyclic aging with different technologies and DOD values

Once the expected lifetimes due to calendric and cycling aging have been estimated, the actual lifetime of a BSS project can be calculated. Thus, the lifetime of BSS project would be determined by the shortest lifetime either because calendric or cycling aging. Table 10 reports the estimated lifetimes for different technologies and DOD values. As observed, the lifetime of Lead-acid and NiCd batteries is limited by their cycling aging, which indicates that the expected lifetime because cycling aging is irrelevant for these technologies since presumably would be earlier replaced; while the calendric aging strongly affects the lifetime of a BSS project based on Li-ion and NaS batteries. Thus, it is estimated that Lead-Acid batteries should be replaced each year if demanding DOD strategies are adopted while NaS batteries could be replaced each 10 years regardless the adopted DOD settings.

Table 10. Calculated lifetimes [years] for various DOD values and BSS technologies because either calendric or cycling aging

DOD	**Technology**			
[%]	**Lead-acid**	**NiCd**	**Li-ion**	**NaS**
50	4	7	5	10
60	3	4	5	10
70	2	3	5	10
80	2	3	5	10
90	1	2	5	10
100	1	2	5	10

Finally, a NPV analysis has been made in order to discern the most suitable BSS project for the NG under study. Table 11 reports the capital, fixed O&M, installation and replacement costs for the different considered technologies [19,45]. These costs have to be properly evaluated over the project lifetime, for that reason, they were not included in the operating horizon stage. In this study, a discount rate of 12% and an inflation rate of 0.27% have been considered to annualize the cash flows and costs. Fig. 14 shows the NPV for the different technologies and DOD strategies analysed for a time horizon of 25 years, which is the estimated lifetime of a PV array and considered an acceptable time horizon for a NG project [32]. It is considered that a BSS system has to be replaced when

its lifetime ends, either by its calendric or cycling aging (see Table 10). The expected cash flows have been calculated as the difference between the objective function with and without BSS (base case). Since the operating cost barely depends on the technology used, the profitability of each project is mainly determined by its fixed costs, lifetime and DOD strategy. As seen, the Lead-acid and NaS technologies resulted the most profitable mainly due to their low capital costs. The usage of these technologies may result on a profitability of ~50000 $ and ~60000 $ in 25 years for DOD = 80% and DOD = 100%, respectively. On the other hand, despite that the daily lowest operating cost was obtained with the usage of NiCd batteries, this technology only results very few profitable (~4000 $) with DOD < 90%. The Li-ion batteries are clearly very few attractive since only a very low profitability (~500 $), is expected at the end of the project life with DOD = 100%.

Table 11 – Capital and O&M costs of various battery technologies

Technology	**Power rating cost ($/kW)**	**Energy rating cost ($/kWh)**	**Fixed O&M cost ($/kW-yr)**	**Installation Cost ($/kWh)**	**Replacement costs ($/kW)**
Lead-acid	200	200	3.81	20	202
NiCd	500	400	12.32	12	617
Li-ion	900	600	7.73	3.6	434
NaS	350	300	4.03	8	211

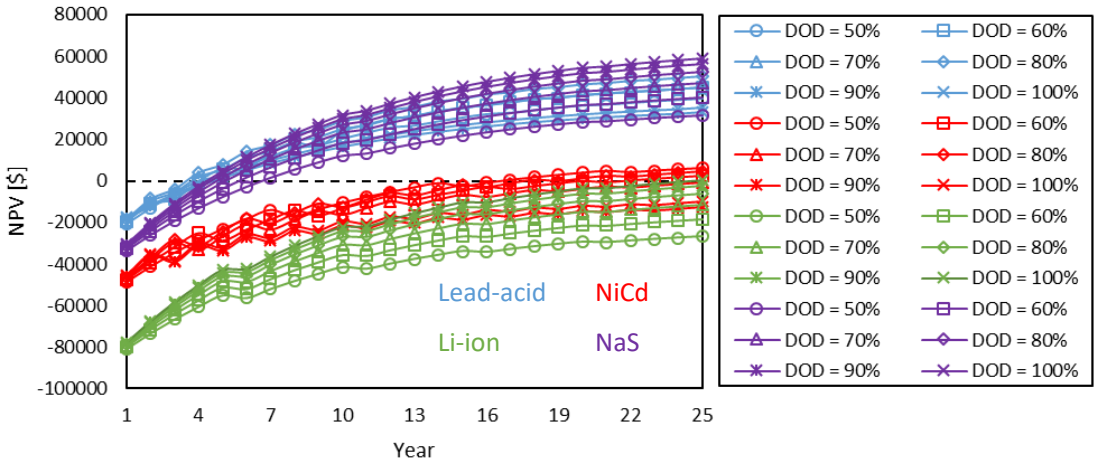

Figure 14. NPV for different technologies and DOD values

6. Further capabilities

In this section, various auxiliaries modifications or approaches that can be incorporated on the original developed algorithm summarized in Fig. 1 are presented. These approaches are either devoted on accelerating the computational process of the developed methodology or further extending their capabilities and are described below.

- Parallelization strategies: although the developed methodology has turned out to be quite efficient (~15 minutes for completely solving the benchmark example on a 64-bit i5-8500F Intel Core personal computer (3 GHz, 8 GB of RAM)), it may entail a high computational effort on larger systems with many variables. In this sense, the main bottleneck of the novel proposal is the day-ahead optimal scheduling algorithm, whose computational burden grows with the complexity of the system (number of variables and handled data). To solve this issue, the developed methodology allows to easily parallelize this tool. For example, for the case study of this paper, one can run each mixed-integer quadratic programming problem for the different DOD strategies and batteries technologies tested, since this problem is totally independent with respect to these parameters. In this sense, the computational time consumed by an average computer would be equivalent to the total time employed on solving just one mixed-integer quadratic problem (~1 minute). Fig. 15 shows a modification of the flowchart of Fig. 3 to incorporate parallelization strategies.

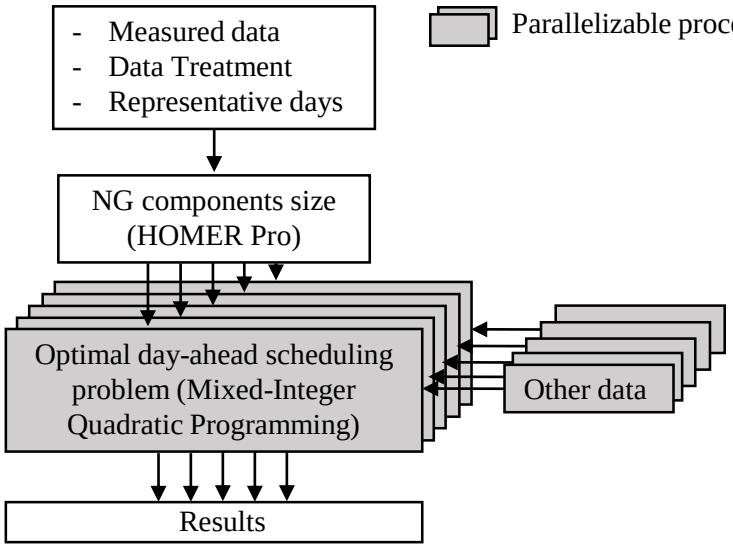

Figure 15. Possible scheme to incorporate parallelization strategies within the developed methodology

- Sensitivity analysis: the developed methodology can be further extended to analyse the impact of some parameters (e.g. O&M costs of the different units). In that sense, the block called should incorporate the different parameters value that would take part on the sensitivity analysis. To evaluate the impact of some generic parameter x, the scheme of Fig. 1 can be easily modified according to the flowchart showed in Fig. 16. As seen, the mixed-integer quadratic programming is repeatedly executed for the different values of the concerned parameter, thus, only an external loop has to be programmed. Intuitively, carrying out a sensitivity analysis suppose an extra computational burden with respect to the original approach, nevertheless, this computational effort may be effectively alleviated by using parallelization strategies such as that described in Fig. 15.

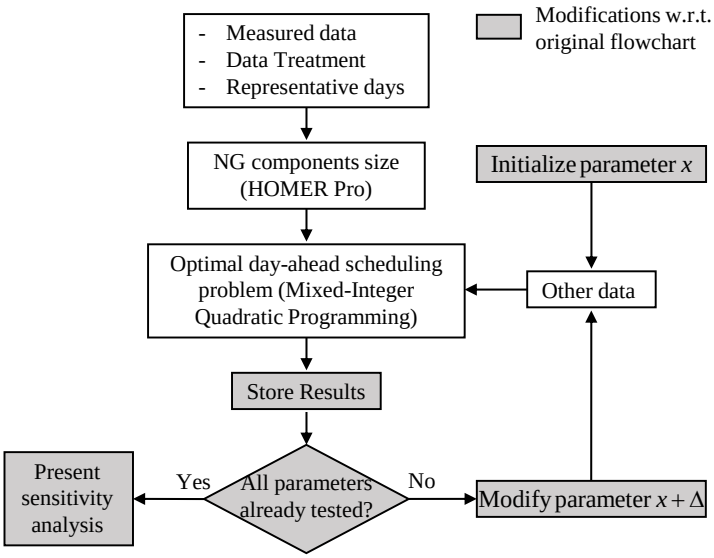

Figure 16. Modification of the original flowchart for carrying out a sensitivity analysis

- Different batteries technologies: the developed methodology also allows to consider that the battery storage bank incorporates different battery technologies (e.g. a battery system formed by NiCd and NaS batteries). To consider this issue, the formulation of the optimal day-ahead scheduling problem has to be slightly modified. More precisely, the variables $p_{r,t}^{BSS,C}$, $p_{r,t}^{BSS,D}$, $\delta_{r,t}^{BSS,C}$, $\delta_{r,t}^{BSS,D}$ and $e_{r,t}^{BSS}$ should be splitted according to the approach schematized in Fig. 17, where it is assumed that k different batteries technologies are incorporated. Regarding the storage system capacity, it can be still selected as it has been done in Section 5.1 (i.e. take the lowest storage capacity), however, the user should predefine what percentage of the total capacity is destined to each technology, which entails that the parameter S^{BSS} has to be also splitted into k parameters. Once it has been done, the constraints and equations (18)-(26) have to be reproduced k times (once per each battery technology).

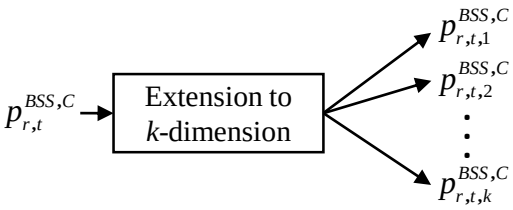

Figure 17. Example of variable division to incorporate different batteries technologies on the same storage bank (the same approach is used for the variables $p_{r,t}^{BSS,D}$, $\delta_{r,t}^{BSS,C}$, $\delta_{r,t}^{BSS,D}$ and $e_{r,t}^{BSS}$ and the different constraints and equations involved)

Results for these approaches are not shown in this paper since their applicability is trivial and result provided are useless. For example, the application of parallelization strategies would have only impact on the computational time while the presentation of the results provided by a sensitivity analysis might lead to very large and unnecessary extension of the paper.

7. Conclusions

This work has developed a novel methodology for comprehensive planning of BSS in NGs and microgrids. The developed framework originally combines different techniques, software and tools, in order to overcome some issues presented by other state-of-art methodologies. In order to validate and illustrate the developed approach, it has been applied to a prospective NG in the region of Cuenca, Ecuador. Results obtained in this case study allows us to conclude that:

1. The developed methodology allows to efficiently and effectively manage with the large amount of measured data and uncertainties brought by renewable generation. To overcome these two issues, clustering techniques have been used in order to characterize the measured data by representative days. Instead of other approaches which use scenarios generation approaches via probability functions, our proposal allows to take advantage of historical data in order to keep faithful to the particularities of each grid and situation. In addition, the total number of

scenarios to generate and probability of each scenario can be easily obtained as by-product from the clustering technique used.

2. The developed framework is able to effectively manage with different time horizons. This interesting feature is achieved by combining different software and tools. Thus, while the software HOMER Pro® is used for planning purposes, other relevant indicators are obtained via a designed day-ahead optimal scheduling tool. This original combination allows to obtain a large amount of helpful and relevant results. Among others, the application of the developed methodology to the case study has allowed to determine the most suitable batteries technology and DOD strategy; project cost through its lifetime; yearly operating cost and lifetime of each battery technology.
3. The developed methodology is quite efficient as demonstrate the computation time employed on solving the case study. The whole algorithm was carried out on an average machine consuming ~15 minutes. In addition, the proposed methodology allows to incorporate parallelization routines in a simply way to speed up the overall process.
4. As illustrative conclusion referring to the particular case study let us comment that, despite the most competitive operating cost was obtained by using NiCd batteries, this technology resulted scarcely profitable due to its high fixed costs. For this same reason, Li-ion technology seems a very few attractive alternative from an economic point of view. On the other hand, Lead-acid and NaS batteries seem profitable solutions for the NG under study. Both technologies presumably offer a profitability ~ 60000 $ in 25 years.

On the light of the results obtained in this study, it can be asserted that this methodology can be straightforward used for similar studies on different kind of grids. It is expected to

confirm to further confirm this aspect in future works carried out by the authors and other researchers on different microgrid and NG layouts.

8. Acknowledgements

The icons used in this article were made by Freepik from www.flaticon.com.

9. References

[1] J.M. Aberilla, A. Gallego-Schmid, L. Stamford, A. Azapagic, Design and environmental sustainability assessment of small-scale off-grid energy systems for remote rural communities, Appl. Energy. 258 (2020) 114004. https://doi.org/10.1016/j.apenergy.2019.114004.

[2] T.L. Nguyen, J.M. Guerrero, G. Griepentrog, A Self-Sustained and Flexible Control Strategy for Islanded DC Nanogrids without Communication Links, IEEE J. Emerg. Sel. Top. Power Electron. 8 (2020) 877–892. https://doi.org/10.1109/JESTPE.2019.2894564.

[3] J. Bae, S. Lee, H. Kim, Comparative study on the economic feasibility of nanogrid and microgrid electrification: The case of Jeju Island, South Korea, Energy Environ. 0 (2020) 1–21. https://doi.org/10.1177/0958305X20923119.

[4] D. Akinyele, Techno-economic design and performance analysis of nanogrid systems for households in energy-poor villages, Sustain. Cities Soc. 34 (2017) 335–357. https://doi.org/10.1016/j.scs.2017.07.004.

[5] A.T. Dahiru, C.W. Tan, Optimal sizing and techno-economic analysis of grid-connected nanogrid for tropical climates of the Savannah, Sustain. Cities Soc. 52 (2020) 101824. https://doi.org/10.1016/j.scs.2019.101824.

[6] M. Nazari-Heris, M.A. Mirzaei, B. Mohammadi-Ivatloo, M. Marzband, S. Asadi, Economic-environmental effect of power to gas technology in coupled electricity and gas systems with price-responsive shiftable loads, J. Clean. Prod. 244 (2020) 118769. https://doi.org/10.1016/j.jclepro.2019.118769.

[7] M. Tostado-Véliz, P. Arévalo, F. Jurado, A comprehensive electrical-gas-hydrogen Microgrid model for energy management applications, Energy Convers. Manag. 228 (2021) 113726. https://doi.org/10.1016/j.enconman.2020.113726.

[8] C.D. Korkas, S. Baldi, I. Michailidis, E.B. Kosmatopoulos, Occupancy-based demand response and thermal comfort optimization in microgrids with renewable energy sources and energy storage, Appl. Energy. 163 (2016) 93–104. https://doi.org/10.1016/j.apenergy.2015.10.140.

[9] C.D. Korkas, S. Baldi, E.B. Kosmatopoulos, Grid-Connected Microgrids: Demand Management via Distributed Control and Human-in-the-Loop Optimization, in: Adv. Renew. Energies Power Technol., Elsevier, 2018: pp. 315–344. https://doi.org/10.1016/B978-0-12-813185-5.00025-5.

[10] M. Tavakoli, F. Shokridehaki, M. Funsho Akorede, M. Marzband, I. Vechiu, E. Pouresmaeil, CVaR-based energy management scheme for optimal resilience and operational cost in commercial building microgrids, Int. J. Electr. Power Energy Syst. 100 (2018) 1–9. https://doi.org/10.1016/j.ijepes.2018.02.022.

[11] M. Tavakoli, F. Shokridehaki, M. Marzband, R. Godina, E. Pouresmaeil, A two stage hierarchical control approach for the optimal energy management in commercial building microgrids based on local wind power and PEVs, Sustain. Cities Soc. 41 (2018) 332–340. https://doi.org/10.1016/j.scs.2018.05.035.

[12] M. Jadidbonab, B. Mohammadi-Ivatloo, M. Marzband, P. Siano, Short-Term Self-Scheduling of Virtual Energy Hub Plant Within Thermal Energy Market, IEEE Trans. Ind. Electron. 68 (2021) 3124–3136. https://doi.org/10.1109/TIE.2020.2978707.

[13] M. Tostado-Véliz, D. Icaza-Alvarez, F. Jurado, A Novel Methodology for Optimal Sizing Photovoltaic-Battery Systems in Smart Homes considering Grid Outages and Demand Response, Renew. Energy 170 (2021) 884-896. https://doi.org/10.1016/j.renene.2021.02.006.

[14] H. Ganjeh Ganjehlou, H. Niaei, A. Jafari, D.O. Aroko, M. Marzband, T. Fernando, A novel techno-economic multi-level optimization in home-microgrids with coalition formation capability, Sustain. Cities Soc. 60 (2020) 102241. https://doi.org/10.1016/j.scs.2020.102241.

[15] D. Burmester, R. Rayudu, W. Seah, D. Akinyele, A review of nanogrid topologies and technologies, Renew. Sustain. Energy Rev. 67 (2017) 760–775. https://doi.org/10.1016/j.rser.2016.09.073.

[16] D. Boroyevich, I. Cvetković, D. Dong, R. Burgos, F. Wang, F. Lee, Future electronic power distribution systems - A contemplative view, in: Proc. Int. Conf. Optim. Electr. Electron. Equipment, OPTIM, 2010: pp. 1369–1380. https://doi.org/10.1109/OPTIM.2010.5510477.

[17] P.P. Kumar, R.P. Saini, Optimization of an off-grid integrated hybrid renewable energy system with different battery technologies for rural electrification in India, J. Energy Storage. 32 (2020) 101912. https://doi.org/10.1016/j.est.2020.101912.

[18] P. P Kumar, R.P. Saini, Optimization of an off-grid integrated hybrid renewable

energy system with various energy storage technologies using different dispatch strategies, Energy Sources, Part A Recover. Util. Environ. Eff. 42 (2020). https://doi.org/10.1080/15567036.2020.1824035.

[19] I. Alsaidan, A. Khodaei, W. Gao, A Comprehensive Battery Energy Storage Optimal Sizing Model for Microgrid Applications, IEEE Trans. Power Syst. 33 (2018) 3968–3980. https://doi.org/10.1109/TPWRS.2017.2769639.

[20] M.H. Mostafa, S.H.E.A. Aleem, S.G. Ali, A.Y. Abdelaziz, P.F. Ribeiro, Z.M. Ali, Robust energy management and economic analysis of microgrids considering different battery characteristics, IEEE Access. 8 (2020) 54751–54775. https://doi.org/10.1109/ACCESS.2020.2981697.

[21] M.B. Eteiba, S. Barakat, M.M. Samy, W.I. Wahba, Optimization of an off-grid PV/Biomass hybrid system with different battery technologies, Sustain. Cities Soc. 40 (2018) 713–727. https://doi.org/10.1016/j.scs.2018.01.012.

[22] S. Paul Ayeng'o, T. Schirmer, K.P. Kairies, H. Axelsen, D. Uwe Sauer, Comparison of off-grid power supply systems using lead-acid and lithium-ion batteries, Sol. Energy. 162 (2018) 140–152. https://doi.org/10.1016/j.solener.2017.12.049.

[23] G. Merei, C. Berger, D.U. Sauer, Optimization of an off-grid hybrid PV-Wind-Diesel system with different battery technologies using genetic algorithm, Sol. Energy. 97 (2013) 460–473. https://doi.org/10.1016/j.solener.2013.08.016.

[24] R.E. Ciez, J.F. Whitacre, Comparative techno-economic analysis of hybrid micro-grid systems utilizing different battery types, Energy Convers. Manag. 112 (2016) 435–444. https://doi.org/10.1016/j.enconman.2016.01.014.

[25] C. Mokhtara, B. Negrou, A. Bouferrouk, Y. Yao, N. Settou, M. Ramadan, Integrated supply–demand energy management for optimal design of off-grid hybrid renewable energy systems for residential electrification in arid climates, Energy Convers. Manag. 221 (2020) 113192. https://doi.org/https://doi.org/10.1016/j.enconman.2020.113192.

[26] S. Dhundhara, Y.P. Verma, A. Williams, Techno-economic analysis of the lithium-ion and lead-acid battery in microgrid systems, Energy Convers. Manag. 177 (2018) 122–142. https://doi.org/10.1016/j.enconman.2018.09.030.

[27] K.L. Tharani, R. Dahiya, Choice of battery energy storage for a hybrid renewable energy system, Turkish J. Electr. Eng. Comput. Sci. 26 (2018) 666–676. https://doi.org/10.3906/elk-1707-350.

[28] C. Liu, J. Jiang, J. Jiang, Z. Zhou, Enhanced Grid-Connected Phase-Locked Loop Based on a Moving Average Filter, IEEE Access. 8 (2020) 5308–5315. https://doi.org/10.1109/ACCESS.2019.2963362.

[29] K. Poncelet, H. Hoschle, E. Delarue, A. Virag, W. Drhaeseleer, Selecting representative days for capturing the implications of integrating intermittent renewables in generation expansion planning problems, IEEE Trans. Power Syst. 32 (2017) 1936–1948. https://doi.org/10.1109/TPWRS.2016.2596803.

[30] Á. García-Cerezo, L. Baringo, R. García-Bertrand, Representative Days for Expansion Decisions in Power Systems, Energies. 13 (2020) 335. https://doi.org/10.3390/en13020335.

[31] K. Poncelet, E. Delarue, D. Six, J. Duerinck, W. D'haeseleer, Impact of the level of temporal and operational detail in energy-system planning models, Appl.

Energy. 162 (2016) 631–643. https://doi.org/10.1016/j.apenergy.2015.10.100.

[32] S. Swaminathan, G.S. Pavlak, J. Freihaut, Sizing and dispatch of an islanded microgrid with energy flexible buildings, Appl. Energy. 276 (2020) 115355. https://doi.org/10.1016/j.apenergy.2020.115355.

[33] E.S. Pinto, L.M. Serra, A. Lázaro, Evaluation of methods to select representative days for the optimization of polygeneration systems, Renew. Energy. 151 (2020) 488–502. https://doi.org/10.1016/j.renene.2019.11.048.

[34] HOMER Pro - Microgrid Software for Designing Optimized Hybrid Microgrids, (n.d.). https://www.homerenergy.com/products/pro/index.html (accessed July 2, 2020).

[35] Gurobi, The fastest solver - Gurobi, 2019. (n.d.). https://www.gurobi.com/ (accessed July 5, 2020).

[36] S. Mandal, B.K. Das, N. Hoque, Optimum sizing of a stand-alone hybrid energy system for rural electrification in Bangladesh, J. Clean. Prod. 200 (2018) 12–27. https://doi.org/10.1016/j.jclepro.2018.07.257.

[37] S.P. Koko, K. Kusakana, H.J. Vermaak, Optimal power dispatch of a grid-interactive micro-hydrokinetic-pumped hydro storage system, J. Energy Storage. 17 (2018) 63–72. https://doi.org/10.1016/j.est.2018.02.013.

[38] L. Alvarado-Barrios, Á. Rodríguez del Nozal, J. Boza Valerino, I. García Vera, J.L. Martínez-Ramos, Stochastic unit commitment in microgrids: Influence of the load forecasting error and the availability of energy storage, Renew. Energy. 146 (2020) 2060–2069. https://doi.org/10.1016/j.renene.2019.08.032.

[39] A. Cano, P. Arévalo, F. Jurado, Energy analysis and techno-economic assessment of a hybrid PV/HKT/BAT system using biomass gasifier: Cuenca-Ecuador case study, Energy. 202 (2020) 117727. https://doi.org/10.1016/j.energy.2020.117727.

[40] M. Faisal, M.A. Hannan, P.J. Ker, A. Hussain, M. Bin Mansor, F. Blaabjerg, Review of energy storage system technologies in microgrid applications: Issues and challenges, IEEE Access. 6 (2018) 35143–35164. https://doi.org/10.1109/ACCESS.2018.2841407.

[41] J.L. Espinoza, L.G. Gonzalez, R. Sempertegui, Micro grid laboratory as a tool for research on non-conventional energy sources in Ecuador, in: 2017 IEEE Int. Autumn Meet. Power, Electron. Comput. ROPEC 2017, Institute of Electrical and Electronics Engineers Inc., 2018: pp. 1–7. https://doi.org/10.1109/ROPEC.2017.8261615.

[42] Hydrological Monitor V1, (n.d.). http://186.42.174.236/HidroInamhiV1/Front-End/ (accessed July 2, 2020).

[43] V.S. Neary, M. Previsic, R.A. Jepsen, M.J. Lawson, Y.-H. Yu, A.E. Copping, A.A. Fontaine, K.C. Hallett, D.K. Murray, SANDIA REPORT Methodology for Design and Economic Analysis of Marine Energy Conversion (MEC) Technologies, 2014. http://www.ntis.gov/help/ordermethods.asp?loc=7-4-0#online (accessed October 12, 2020).

[44] S. Saneifard, N.R. Prasad, H.A. Smolleck, A fuzzy logic approach to unit commitment, IEEE Trans. Power Syst. 12 (1997) 988–995. https://doi.org/10.1109/59.589804.

[45] B. Zakeri, S. Syri, Electrical energy storage systems: A comparative life cycle cost

analysis, Renew. Sustain. Energy Rev. 42 (2015) 569–596. https://doi.org/10.1016/J.RSER.2014.10.011.

[46] K. Mongird, V. Fotedar, V. Viswanathan, V. Koritarov, P. Balducci, B. Hadjerioua, J. Alam, Energy Storage Technology and Cost Characterization Report, 2019. https://www.energy.gov/sites/prod/files/2019/07/f65/Storage Cost and Performance Characterization Report_Final.pdf (accessed July 5, 2020).